

6 Elastic Scattering off Nucleons

6.1 Form Factors of the Nucleons

Elastic electron scattering off the lightest nuclei, hydrogen and deuterium, yields information about the nuclear building blocks, the proton and the neutron. Certain subtleties have, however, to be taken into account in any discussion of these experiments.

Recoil. As we will soon see, nucleons have a radius of about 0.8 fm. Their study therefore requires energies from some hundred MeV up to several GeV. Comparing these energies with the mass of the nucleon $M \approx 938 \text{ MeV}/c^2$, we see that they are of the same order of magnitude. Hence the target recoil can no longer be neglected. In the derivation of the cross-sections (5.33) and (5.39) we “prepared” for this by using E' rather than E . On top of this, however, the phase space density dn/dE_f in (5.20) must be modified. We so eventually find an additional factor of E'/E in the Mott cross-section [Pe87]:

$$\left(\frac{d\sigma}{d\Omega}\right)_{\text{Mott}} = \left(\frac{d\sigma}{d\Omega}\right)_{\text{Mott}}^* \cdot \frac{E'}{E}. \quad (6.1)$$

Since the energy loss of the electron due to the recoil is now significant, it is no longer possible to describe the scattering in terms of a three-momentum transfer. Instead the four-momentum transfer, whose square is Lorentz-invariant:

$$\begin{aligned} q^2 &= (p - p')^2 = 2m_e^2 c^2 - 2(E E' / c^2 - |\mathbf{p}||\mathbf{p}'| \cos \theta) \\ &\approx \frac{-4EE'}{c^2} \sin^2 \frac{\theta}{2}, \end{aligned} \quad (6.2)$$

must be used. In order to only work with positive quantities we define:

$$Q^2 = -q^2. \quad (6.3)$$

In the Mott cross-section, q^2 must be replaced by q^2 or Q^2 .

Magnetic moment. We must now not only take the interaction of the electron with the nuclear charge into account, but also we have to consider the interaction between the current of the electron and the nucleon's magnetic moment.

The magnetic moment of a charged, spin-1/2 particle which does not possess any internal structure (a Dirac particle) is given by

$$\mu = g \cdot \frac{e}{2M} \cdot \frac{\hbar}{2} \quad (6.4)$$

where M is the mass of the particle and the $g = 2$ factor is a result of relativistic quantum mechanics (the Dirac equation). The magnetic interaction is associated with a flip of the spin of the nucleon. An argument analogous to that of Sect. 5.3 is applicable here: scattering through 0° is not consistent with conservation of both angular momentum and helicity and scattering through 180° is preferred. The magnetic interaction thus introduces a factor into the interaction which, analogously to (5.39), contains a factor of $\sin^2 \frac{\theta}{2}$. With $\sin^2 \frac{\theta}{2} = \cos^2 \frac{\theta}{2} \cdot \tan^2 \frac{\theta}{2}$ we obtain for the cross-section:

$$\left(\frac{d\sigma}{d\Omega} \right)_{\text{spin } 1/2}^{\text{point}} = \left(\frac{d\sigma}{d\Omega} \right)_{\text{Mott}} \cdot \left[1 + 2\tau \tan^2 \frac{\theta}{2} \right], \quad (6.5)$$

where

$$\tau = \frac{Q^2}{4M^2c^2}. \quad (6.6)$$

The 2τ factor can be fairly easily made plausible: the matrix element of the interaction is proportional to the magnetic moment of the nucleon (and thus to $1/M$) and to the magnetic field which is produced at the target in the scattering process. Integrated over time, this is then proportional to the deflection of the electron (i.e., to the momentum transfer Q). These quantities then enter the cross-section quadratically.

The magnetic term in (6.5) is large at high four-momentum transfers Q^2 and if the scattering angle θ is large. This additional term causes the cross-section to fall off less strongly at larger scattering angles and a more isotropic distribution is found than the electric interaction alone would produce.

Anomalous magnetic moment. For charged Dirac-particles the g -factor in (6.4) should be exactly 2, while for neutral Dirac particles the magnetic moment should vanish. Indeed measurements of the magnetic moments of electrons and muons yield the value $g = 2$, up to small deviations. These last are caused by quantum electrodynamical processes of higher order, which are theoretically well understood.

Nucleons, however, are not Dirac particles since they are made up of quarks. Therefore their g -factors are determined by their sub-structure. The values measured for protons and neutrons are:

$$\mu_{\text{p}} = \frac{g_{\text{p}}}{2} \mu_{\text{N}} = +2.79 \cdot \mu_{\text{N}} , \quad (6.7)$$

$$\mu_{\text{n}} = \frac{g_{\text{n}}}{2} \mu_{\text{N}} = -1.91 \cdot \mu_{\text{N}} , \quad (6.8)$$

where the nuclear magneton μ_{N} is:

$$\mu_{\text{N}} = \frac{e\hbar}{2M_{\text{p}}} = 3.1525 \cdot 10^{-14} \text{ MeV T}^{-1} . \quad (6.9)$$

Charge and current distributions can be described by form factors, just as in the case of nuclei. For nucleons, two form factors are necessary to characterise both the electric and magnetic distributions. The cross-section for the scattering of an electron off a nucleon is described by the *Rosenbluth formula* [Ro50]:

$$\left(\frac{d\sigma}{d\Omega} \right) = \left(\frac{d\sigma}{d\Omega} \right)_{\text{Mott}} \cdot \left[\frac{G_{\text{E}}^2(Q^2) + \tau G_{\text{M}}^2(Q^2)}{1 + \tau} + 2\tau G_{\text{M}}^2(Q^2) \tan^2 \frac{\theta}{2} \right] . \quad (6.10)$$

Here $G_{\text{E}}(Q^2)$ and $G_{\text{M}}(Q^2)$ are the *electric and magnetic form factors* both of which depend upon Q^2 . The measured Q^2 -dependence of the form factors gives us information about the radial charge distributions and the magnetic moments. The limiting case $Q^2 \rightarrow 0$ is particularly important. In this case G_{E} coincides with the electric charge of the target, normalised to the elementary charge e ; and G_{M} is equal to the magnetic moment μ of the target, normalised to the nuclear magneton. The limiting values are:

$$\begin{aligned} G_{\text{E}}^{\text{p}}(Q^2 = 0) &= 1 & G_{\text{E}}^{\text{n}}(Q^2 = 0) &= 0 \\ G_{\text{M}}^{\text{p}}(Q^2 = 0) &= 2.79 & G_{\text{M}}^{\text{n}}(Q^2 = 0) &= -1.91 . \end{aligned} \quad (6.11)$$

In order to independently determine $G_{\text{E}}(Q^2)$ and $G_{\text{M}}(Q^2)$ the cross-sections must be measured at fixed values of Q^2 , for various scattering angles θ (i. e., at different beam energies E). The measured cross-sections are then divided by the Mott cross-sections. If we display the results as a function of $\tan^2(\theta/2)$, then the measured points form a straight line (Fig. 6.1), in accordance with the Rosenbluth formula. $G_{\text{M}}(Q^2)$ is then determined by the slope of the line, and the intercept $(G_{\text{E}}^2 + \tau G_{\text{M}}^2)/(1 + \tau)$ at $\theta = 0$ then yields $G_{\text{E}}(Q^2)$. If we perform this analysis for various values of Q^2 we can obtain the Q^2 dependence of the form factors.

Measurements of the electromagnetic form factors right up to very high values of Q^2 were carried out mainly in the late sixties and early seventies at accelerators such as the linear accelerator SLAC in Stanford. Figure 6.2 shows the Q^2 dependence of the two form factors for both protons and neutrons.

It turned out that the proton electric form factor and the magnetic form factors of both the proton and the neutron fall off similarly with Q^2 . They can be described to a good approximation by a so-called *dipole fit*:

$$G_{\text{E}}^{\text{p}}(Q^2) = \frac{G_{\text{M}}^{\text{p}}(Q^2)}{2.79} = \frac{G_{\text{M}}^{\text{n}}(Q^2)}{-1.91} = G^{\text{dipole}}(Q^2)$$

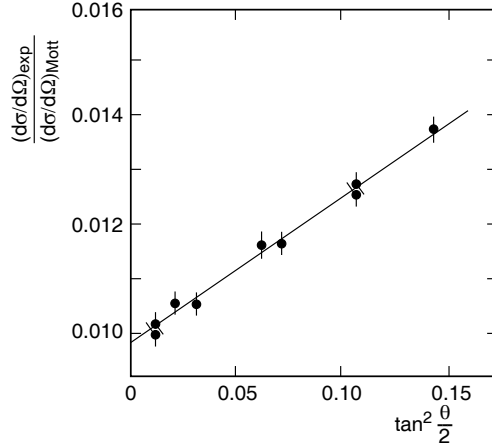


Fig. 6.1. Ratio of the measured cross-section and the Mott cross-section $\sigma_{\text{exp}}/\sigma_{\text{Mott}}$ as a function of $\tan^2\theta/2$ at a four-momentum transfer of $Q^2 = 2.5 \text{ GeV}^2/c^2$ [Ta67].

where
$$G^{\text{dipole}}(Q^2) = \left(1 + \frac{Q^2}{0.71 (\text{GeV}/c)^2}\right)^{-2}. \quad (6.12)$$

The neutron appears from the outside to be electrically neutral and it therefore has a very small electric form factor.

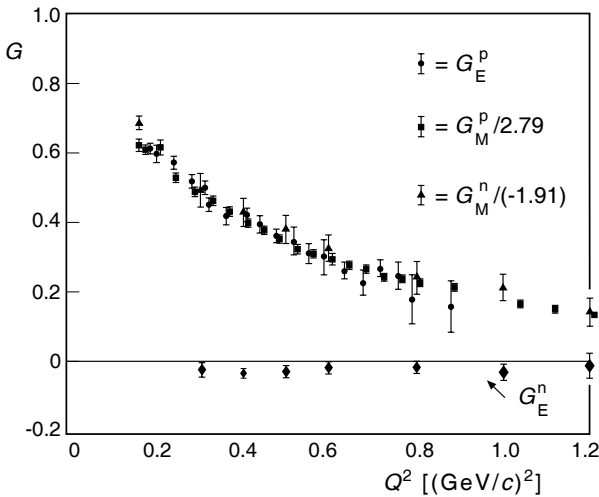


Fig. 6.2. Proton and neutron electric and magnetic form factors as functions of Q^2 . The data points are scaled by the factors noted in the diagram so that they coincide and thus more clearly display the global dipole-like behaviour [Hu65].

We may obtain the nucleons' charge distributions and magnetic moments from the Q^2 dependence of the form factors, just as we saw could be done for nuclei. The interpretation of the form factors as the Fourier transform of the static charge distribution is, however, only correct for small values of Q^2 , since only then are the three- and four-momentum transfers approximately equal. The observed dipole form factor (6.12) corresponds to a charge distribution which falls off exponentially (cf. Fig. 5.6):

$$\varrho(r) = \varrho(0) e^{-ar} \quad \text{with } a = 4.27 \text{ fm}^{-1}. \quad (6.13)$$

Nucleons are, we see, neither point-like particles nor homogeneously charged spheres, but rather quite diffuse systems.

The mean square radii of the charge distribution in the proton and of the magnetic moment distributions in the proton and the neutron are similarly large. They may be found from the slope of $G_{E,M}(Q^2)$ at $Q^2 = 0$. The dipole fit yields:

$$\begin{aligned} \langle r^2 \rangle_{\text{dipole}} &= -6\hbar^2 \left. \frac{dG^{\text{dipole}}(Q^2)}{dQ^2} \right|_{Q^2=0} = \frac{12}{a^2} = 0.66 \text{ fm}^2, \\ \sqrt{\langle r^2 \rangle_{\text{dipole}}} &= 0.81 \text{ fm}. \end{aligned} \quad (6.14)$$

Precise measurements of the form factors at small values of Q^2 show slight deviations from the dipole parametrisation. The slope at $Q^2 \rightarrow 0$ determined from these data yields the present best value [Bo75] of the charge radius of the proton:

$$\sqrt{\langle r^2 \rangle_{\text{p}}} = 0.862 \text{ fm}. \quad (6.15)$$

Determining the neutron electric form factor is rather difficult: targets with free neutrons are not available and so information about $G_{\text{E}}^{\text{n}}(Q^2)$ must be extracted from electron scattering off deuterons. In this case it is necessary to correct the measured data for the effects of the nuclear force between the proton and the neutron. However, an alternative, elegant approach has been developed to determine the charge radius of the free neutron. Low-energy neutrons from a nuclear reactor are scattered off electrons in an atomic shell and the so-ejected electrons are then measured. This reaction corresponds to electron-neutron scattering at small Q^2 . The result of these measurements is [Ko95]:

$$-6\hbar^2 \left. \frac{dG_{\text{E}}^{\text{n}}(Q^2)}{dQ^2} \right|_{Q^2=0} = -0.113 \pm 0.005 \text{ fm}^2. \quad (6.16)$$

The neutron, therefore, only appears electrically neutral from the outside. Its interior contains electrically charged constituents which also possess magnetic moments. Since both the charges and their magnetic moments contribute to the electric form factor, we cannot separate their contributions in a Lorentz invariant fashion. Comparisons with model calculations show that, locally inside the neutron, the charges of the constituents almost completely cancel, which also follows naturally from the measured value (6.16).

6.2 Quasi-elastic Scattering

In Sect. 6.1 we considered the elastic scattering of electrons off free protons (neutrons) at rest. In this reaction for a given beam energy E and at a fixed scattering angle θ scattered electrons always have a definite scattering energy E' which is given by (5.15):

$$E' = \frac{E}{1 + \frac{E}{Mc^2}(1 - \cos\theta)}. \quad (6.17)$$

Repeating the scattering experiment at the same beam energy and at the same detector angle, but now off a nucleus containing several nucleons, a more complicated energy spectrum is observed. Figure 6.3 shows a spectrum of electrons which were scattered off a thin H_2O target, i. e., some were scattered off free protons, some off oxygen nuclei.

The narrow peak observed at $E' \approx 160$ MeV stems from elastic scattering off the free protons in hydrogen. Superimposed is a broad distribution with a maximum shifted a few MeV towards smaller scattering energies. This part of the spectrum may be identified with the scattering of electrons off individual nucleons within the ^{16}O nucleus. This process is called *quasi-elastic scattering*. The sharp peaks at high energies are caused by scattering off the ^{16}O nucleus as a whole (cf. Fig. 5.9). At the left side of the picture, the tail of the Δ -resonance can be recognised, this will be discussed in Sect. 7.1.

Both the shift and the broadening of the quasi-elastic spectrum contain information about the internal structure of atomic nuclei. In the *impulse approximation* we assume that the electron interacts with a single nucleon. The

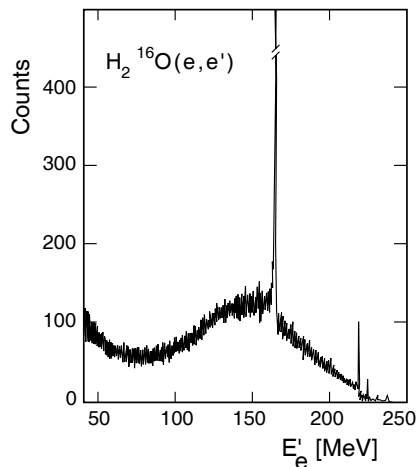
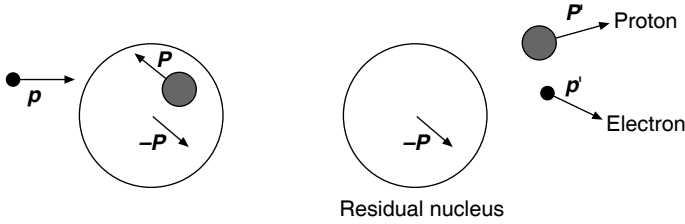


Fig. 6.3. Energy spectrum of electrons scattered off a thin H_2O target. The data were taken at the linear accelerator MAMI-A in Mainz at a beam energy of 246 MeV and at a scattering angle of 148.5° . (Courtesy of J. Friedrich, Mainz)

nucleon is knocked out of the nuclear system by the scattering process without any further interactions with the remaining nucleons in the nucleus. The shift of the maximum in the energy of the scattered electrons towards lower energies is due to the energy needed to remove the nucleon from the nucleus. From the broadening of the maximum, compared to elastic scattering off free protons in the hydrogen atom, we conclude that the nucleus is not a static object with locally fixed nucleons. The nucleons rather move around “quasi-freely” within the nucleus. This motion causes a change in the kinematics compared to scattering off a nucleon at rest.

Let us consider a bound nucleon moving with momentum \mathbf{P} in an effective average nuclear potential of strength S . This nucleon’s binding energy is then $S - \mathbf{P}^2/2M$. We neglect residual interactions with other nucleons, and the kinetic energy of the remaining nucleus and consider the scattering of an electron off this nucleon.



In this case, the following kinematic connections apply:

$$\begin{aligned} \mathbf{p} + \mathbf{P} &= \mathbf{p}' + \mathbf{P}' && \text{momentum conservation in the e-p system} \\ \mathbf{P}' &= \mathbf{q} + \mathbf{P} && \text{momentum conservation in the } \gamma\text{-p system} \\ E + E_p &= E' + E'_p && \text{energy conservation in the e-p system} \end{aligned}$$

The energy transfer ν from the electron to the proton for $E, E' \gg m_e c^2$ and $|\mathbf{P}|, |\mathbf{P}'| \ll Mc$ is given by:

$$\begin{aligned} \nu &= E - E' = E'_p - E_p = \left(Mc^2 + \frac{\mathbf{P}'^2}{2M} \right) - \left(Mc^2 + \frac{\mathbf{P}^2}{2M} - S \right) \\ &= \frac{(\mathbf{P} + \mathbf{q})^2}{2M} - \frac{\mathbf{P}^2}{2M} + S = \frac{\mathbf{q}^2}{2M} + S + \frac{2|\mathbf{q}||\mathbf{P}|\cos\alpha}{2M}, \end{aligned} \quad (6.18)$$

where α is the angle between \mathbf{q} and \mathbf{P} . We now assume that the motion of the nucleons within the nucleus is isotropic (i. e. a spherically symmetric distribution). This leads to a symmetric distribution for ν around an average value:

$$\nu_0 = \frac{\mathbf{q}^2}{2M} + S \quad (6.19)$$

with a width of

$$\sigma_\nu = \sqrt{\langle (\nu - \nu_0)^2 \rangle} = \frac{|\mathbf{q}|}{M} \sqrt{\langle \mathbf{P}^2 \cos^2 \alpha \rangle} = \frac{|\mathbf{q}|}{M} \sqrt{\frac{1}{3} \langle \mathbf{P}^2 \rangle}. \quad (6.20)$$

Table 6.1. Fermi momentum P_F and effective average potential S for various nuclei. These values were obtained from an analysis of quasi-elastic electron scattering at beam energies between 320 MeV and 500 MeV and at a fixed scattering angle of 60° [Mo71, Wh74]. The errors are approximately 5 MeV/c (P_F) and 3 MeV (S).

Nucleus	${}^6\text{Li}$	${}^{12}\text{C}$	${}^{24}\text{Mg}$	${}^{40}\text{Ca}$	${}^{59}\text{Ni}$	${}^{89}\text{Y}$	${}^{119}\text{Sn}$	${}^{181}\text{Ta}$	${}^{208}\text{Pb}$
P_F [MeV/c]	169	221	235	249	260	254	260	265	265
S [MeV]	17	25	32	33	36	39	42	42	44

Fermi momentum. As we will discuss in Sect. 17.1, the nucleus can be described as a *Fermi gas* in which the nucleons move around like quasi-free particles. The *Fermi momentum* P_F is related to the mean square momentum by (cf. 17.9):

$$P_F^2 = \frac{5}{3} \langle \mathbf{P}^2 \rangle. \quad (6.21)$$

An analysis of quasi-elastic scattering off different nuclei can thus determine the effective average potential S and the Fermi momentum P_F of the nucleons.

Studies of the A -dependence of S and P_F were first carried out in the early seventies. The results of the first systematic analysis are shown in Table 6.1 and can be summarised as follows:

- The effective average nuclear potential S increases continuously with the mass number A , varying between 17 MeV in Li to 44 MeV in Pb.
- Apart from in the lightest nuclei, the Fermi momentum is nearly independent of A and is:

$$P_F \approx 250 \text{ MeV}/c. \quad (6.22)$$

This behaviour is consistent with the Fermi gas model. The density of nuclear matter is independent of the mass number except for in the lightest nuclei.

6.3 Charge Radii of Pions and Kaons

The charge radii of various other particles can also be measured by the same method that was used for the neutron. For example those of the π -meson [Am84] and the K-meson [Am86], particles which we will introduce in Sect. 8.2. High-energy mesons are scattered off electrons in the hydrogen atom. The form factor is then determined by analysing the angular distribution of the ejected electrons. Since the pion and the kaon are spin-0 particles, they have an electric but not a magnetic form factor.

The Q^2 -dependence of these form factors is shown in Fig. 6.4. Both can be described by a *monopole form factor*:

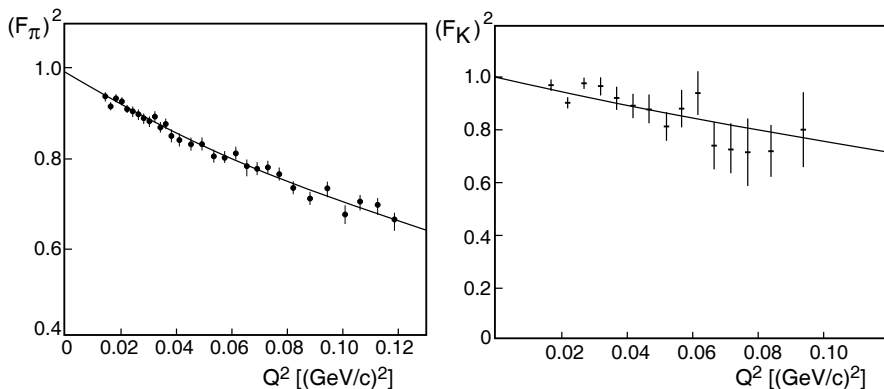


Fig. 6.4. Pion and kaon form factors as functions of Q^2 (from [Am84] and [Am86]). The solid lines correspond to a monopole form factor, $(1 + Q^2/a^2\hbar^2)^{-1}$.

$$G_E(Q^2) = (1 + Q^2/a^2\hbar^2)^{-1} \quad \text{with} \quad a^2 = \frac{6}{\langle r^2 \rangle}. \quad (6.23)$$

The slopes near the origin yield the mean square charge radii:

$$\begin{aligned} \langle r^2 \rangle_\pi &= 0.44 \pm 0.02 \text{ fm}^2 & ; & \quad \sqrt{\langle r^2 \rangle_\pi} = 0.67 \pm 0.02 \text{ fm} \\ \langle r^2 \rangle_K &= 0.34 \pm 0.05 \text{ fm}^2 & ; & \quad \sqrt{\langle r^2 \rangle_K} = 0.58 \pm 0.04 \text{ fm} . \end{aligned}$$

We see that the pion and the kaon have a different charge distribution than the proton, in particular it is less spread out. This may be understood as a result of the different internal structures of these particles. We will see in Chap. 8 that the proton is composed of three quarks, while the pion and kaon are both composed of a quark and an antiquark.

The kaon has a smaller radius than that of the pion. This can be traced back to the fact that the kaon, in contrast to the pion, contains a heavy quark (an s-quark). In Sect. 13.5 we will demonstrate in a heavy quark–antiquark system that the radius of a system of quarks decreases if the mass of its constituents increases.

Problems

1. Electron radius

Suppose one wants to obtain an upper bound for the electron's radius by looking for a deviation from the Mott cross-section in electron-electron scattering. What centre of mass energy would be necessary to set an upper limit on the radius of 10^{-3} fm?

2. Electron-pion scattering

State the differential cross-section, $d\sigma/d\Omega$, for elastic electron-pion scattering. Write out explicitly the Q^2 dependence of the form factor part of the cross-section in the limit $Q^2 \rightarrow 0$ assuming that $\langle r^2 \rangle_\pi = 0.44 \text{ fm}^2$.